ISSN 1069-3513, Izvestiya, Physics of the Solid Earth, 2009, Vol. 45, No. 6, pp. 482–494. © Pleiades Publishing, Ltd., 2009.
Original Russian Text © D. M. Pechersky, D. K. Nurgaliev, Z. V. Sharonova, 2009, published in Fizika Zemli, 2009, No. 6, pp. 20–31.

Magnetic Properties of the Boundary Layer at the Cretaceous/Tertiary Boundary in the Gams Section, Eastern Alps, Austria

D. M. Pechersky[a], D. K. Nurgaliev[b], and Z. V. Sharonova[a]

[a] *Institute of Physics of the Earth, Russian Academy of Sciences, ul. Bol'shaya Gruzinskaya 10, Moscow, 123995 Russia*
[b] *Kazan State University, ul. Lenina 18, Kazan, 420008 Tatarstan, Russia*

Received October 18, 2007

Abstract—The paper is concerned with the detailed sectional petromagnetic study of boundary clay in four 1A, 1B, 2A, and 2B Gams sections (in Austria). The composition of basic magnetic minerals in the boundary clay of all sections is similar. They are composed of iron hydroxides, hemoilmenite, titanomagnetite, magnetite, hematite, and iron. The difference is the presence in the Gams-1 section of metallic nickel, which is absent in the Gams-2 section, and the presence in the latter of iron sulfides of the pyrite type. Grains of titanomagnetite and ilmenite, connected with volcanic activity, are nonuniformly distributed in the boundary layer, which indicates their irregular precipitation in time. The ensemble of magnetic grains is characterized by high coercitivity. The boundary layer is characterized by an increased content of iron hydroxides. This effect is a global phenomenon and is irrelevant to the local physicogeographical conditions. Such a characteristic of impact events as the particles of metallic iron is almost absent in the boundary layer.

PACS numbers: 91.25.F; 91.25.St

DOI: 10.1134/S1069351309060020

INTRODUCTION

According to numerous data, the Mesozoic/Cenozoic boundary is characterized by an increase in magnetic susceptibility. Until recently, first, only the behavior of magnetic susceptibility of sediments near the Cretaceous/Tertiary boundary was analyzed and other magnetic properties were scarcely studied and, second, the boundary layer itself was not investigated in detail. The first deficiency was compensated by the detailed magneto-mineralogical and magneto-lithologic studies executed recently of the epicontinental deposits outcropping on land near the Cretaceous/Tertiary boundary: Koshak (Mangyshlak) [Pechersky et al., 2006], Gams (Austria) [Grachev et al., 2005; Pechersky et al., 2006], Teplovka and Klyuchi (the Volga Region) [Molostovsky et al., 2006], and Tetritskaro (Georgia) [Adamia et al., 1993].

The present paper belongs to the cycle of petromagnetic studies of sediments near the Mesozoic/Cenozoic (Cretaceous/Tertiary) boundary and is concerned with the detailed sectional magneto-mineralogical and magneto-lithologic study of the boundary layer in the epicontinental deposits of Gams sections (Austria), where according to the data presented in [Lahodynsky, 1988] along the Gams River and its confluents near the Gams village the deposits are outcropped, which include the Cretaceous/Tertiary boundary. The samples were selected by A.F. Grachev and O.A. Korchagin in two outcrops Gams-1A and Gams-1B, as well as in Gams-2A and Gams-2B, located at a distance of ~0.5 km. We do not consider the description of these sections, which is carried out in detail in the papers mentioned above. In the present work, the boundary clays of the Gams-2A section, where the thickness of the boundary layer reaches 6 cm (Fig. 1a) and the Gams-2B section with a thickness of 2 cm (Fig. 1b), were subjected to a sectional study.

It should be noted that in all previously studied sections the boundary layer is characterized by the anomalous peak of paramagnetic magnetization and magnetic susceptibility, caused by the high total iron content, which is contained, first of all, in hydroxides, both paramagnetic and ferromagnetic (goethite), i.e., beginning from the boundary layer, an abrupt rise in the accumulation of iron sediments occurs. This is clearly common for the boundary layer (the Cretaceous/Tertiary boundary) of all sections studied [Pechersky, 2007]. Direct correlation is observed between the goethite content and the paramagnetic magnetization (Fig. 2). The goethite content and the value of paramagnetic magnetization are determined independently; therefore this correlation demonstrates their close interrelation, and is indicative of the fact that the paramagnetic material consists primarily of iron hydroxides. Consequently, enrichment by iron hydroxides both in the paramag-

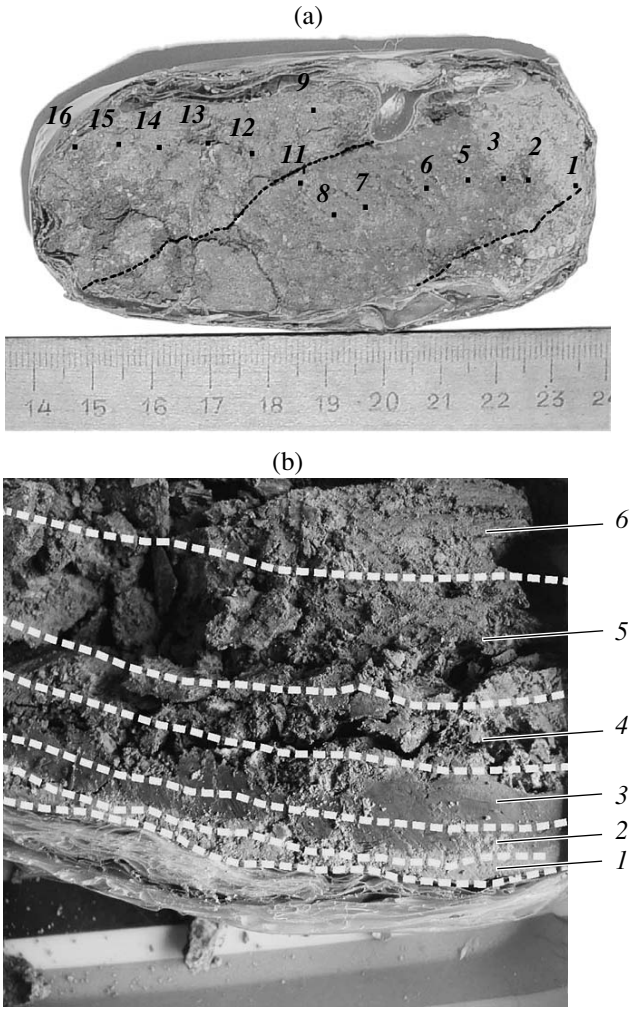

Fig. 1. Photographic illustration of samples of the boundary clay. (a) Rock sample from the Gams-2A section. The sampling points of specimens for studying the magnetic properties are marked and numbered. The level boundaries in the boundary layer are shown by black dotted lines. The apparent thickness of boundary layer is 36 mm. (b) Rock sample from the Gams-2B section. The apparent thickness of the boundary layer is ~50 mm. The sampling points are indicated by numbers *1*, *2*, *3*, *4*, and *5*. The sampling points from the Gams-1B section correspond to them: J_0, J_1, J_2, J_3, and J_{top} (but there the total thickness of the boundary layer is ~20 mm). The level boundaries in the boundary layer of the Gams-2B section, from which the samples are taken, are depicted by white dotted lines.

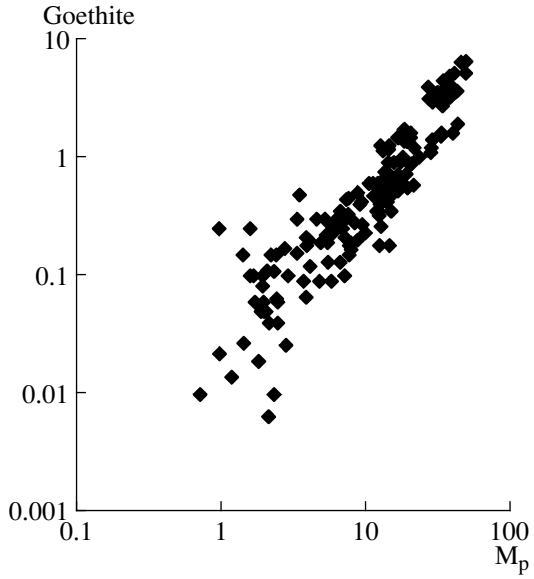

Fig. 2. Correlation of the paramagnetic magnetization $M_p$and the percentage composition of ferromagnetic iron hydroxides (goethite) in sediments according to the data [Pechersky et al., 2006a; 2006b; Molostovsky et al., 2006; Pechersky, 2007] (logarithmic scale across of the both axes).

netic and weak ferromagnetic form, regularly occurs at the Cretaceous/Tertiary boundary.

The distribution of magnetic minerals is different, and their confinement to the boundary layer is not observed. The magnetite content varies approximately from 0.0005 to 0.02%, being partly consistent with the lithologic patterns of the sections: it has higher concentrations in the sandy-clayey deposits. The magnetite content does not fit the regular pattern of the Cretaceous/Tertiary boundary. Lithologic control is even less efficient in the accumulation of the titanomagnetite and metallic iron grains. In the upper part of the boundary layer of the Gams-1 section metallic nickel and its alloy with iron are identified in the single fragments.

It is of interest to compare the data obtained in the present work on Gams-2A and Gams-2B sections with the previously obtained data on Gams-1 section. Therefore, we briefly recall the data on the boundary layer of the Gams-1 section [Grachev et al., 2005; Pechersky et al., 2006]. The thermomagnetic and microprobe analysis of the boundary layer with a thickness of about 2 cm are carried out at six levels. At the bottom of the layer (level *1*) the relatively increased concentration of titanomagnetite grains is observed, which contain 20–23% of TiO_2 that is characteristic for titanomagnetites from basalts. Upwards (levels *2* and *3*), the content of magnetic minerals sharply falls approximately by a factor of 15–20 in comparison with level *1*, and here single grains of metallic iron, magnetite, titanomagnetite, and ilmenite are identified. At level *4*, *metallic nickel* (its contribution in the magnetization intensity predominates), magnetite and iron are identified. The total content of magnetic minerals is approximately 15 times less than their content at level *1*. At level *5*, magnetite and hemoilmenite are identified, a grain of nickel with awaruite inclusions is discovered. At the uppermost part of the boundary layer (level *6*), nickel and titanomagnetite are recorded. The presence of both of them is confirmed by the microprobe data. Such enrichment by grains of nickel is local, since nickel was not discovered in any of other fragments from level *6*, as well as in the entire boundary layer.

METHODS OF PETROMAGNETIC STUDIES

Petromagnetic studies include the measurement of the specific magnetic susceptibility χ, hysteresis characteristics, and anisotropy A_χ and A_{rs}. For the measurement of χ and anisotropy, cubes with an edge of 2 cm were used, the remaining measurements were carried out with fragments of arbitrary shapes with a size of smaller than 10 mm^3, and a weight of less than 0.2 g. Magnetic susceptibility was measured on a KLY-2 magnetic susceptibility meter, the remanent magnetization was measured on a JR-4 magnetometer, the hysteresis characteristics of the samples were investigated with the help of a coercive spectrometer [Burov et al., 1986; Yasonov et al., 1998]. The specific remanent saturation magnetization (M_{rs}), the specific saturation magnetization minus paramagnetic + diamagnetic components (M_s), the coercive force minus the influence of paramagnetic + diamagnetic components (H_c), and the remanent coercive force (H_{cr}) were determined from the magnetization curves.

The ensemble of magnetic minerals, which are present in the samples, is analyzed with the help of the coercive spectra of the normal remanent magnetization [Sholpo, 1977].

The thermomagnetic analysis of rock samples is carried out. The thermomagnetic measurements were conducted on the Curie express balance [Burov et al., 1986], where the temperature dependence of inductive magnetization with the heating rate of 100°C per minute was measured. The thermomagnetic analysis was conducted in a constant magnetic field with an intensity of 200 or 500 mT. In a number of samples the field of saturation is higher, so that a certain inductive magnetization $M_i(T)$ was actually measured, which is the sum of the saturation magnetization (M_s) and the paramagnetic magnetization (M_p) for such magnetic minerals as magnetite, titanomagnetite, hemoilmenite and iron, and the high magnetic field of saturation probably relates to the part of the grains of hemoilmenite and ferromagnetic hydroxides of iron. For all samples the curves of $M_i(T)$ of the first and repeated heating up to 800°C were obtained.

The concentration of magnetite, titanomagnetite, iron, hemoilmenite, and goethite in the samples are evaluated, for which the contribution in the value M_i of the particular magnetic mineral was determined from the curve $M_i(T)$, and this value was divided by the specific saturation magnetization of this mineral. The following M_s values were accepted: ~90 A m^2/kg for magnetite and titanomagnetite, ~200 Am^2/kg for iron, ~4 A m^2/kg for hemoilmenite with T_C higher than 300°C, ~10 Am^2/kg for hemoilmenite with T_C ~250–260°C, and for goethite, the specific saturation magnetization of which varies from 0.02 to 0.5 A m^2/kg, and an average value M_s = 0.25 Am^2/kg is accepted. It is obvious that the obtained estimates of the content of goethite and hemoilmenite are the lower limit of the content of iron hydroxides, hemoilmenite and ilmenite in the samples studied. In the samples of clays of the boundary layer of the Gams-2 section the grains of pyrite and arsenopyrite are identified. Under heating, such minerals are oxidized and magnetite is formed. From the quantity of newly-formed magnetite we make an approximate estimate (the lower limit) of the concentration of Fe-sulfides of the pyrite and arsenopyrite type.

According to the data of magnetic measurements we determined the paramagnetic magnetization of the samples studied.

$$M_p + M_d = M_{20},$$

$$0.274M_p + M_d = M_{800},$$

where M_p is the paramagnetic magnetization at room temperature in the magnetic field 500 mT, M_d is the diamagnetic magnetization at room temperature in the magnetic field 500 mT, diamagnetic magnetization practically does not depend on temperature [Vonsovskii, 1971], M_{20} is the "total" paramagnetic + diamagnetic magnetization (which is determined from the curve of the isothermal magnetization of sample at room temperature in the magnetic field, which is higher than the saturation field of the magnetically ordered (magnetic) minerals, which are present in the sample), and M_{800} is the magnetization of the sample at a temperature of 800° measured in the same field as M_{20}. The multiplier $0.274M_p$ is the ratio of temperatures 295 K/1075 K (the Curie–Weiss law).

RESULTS OF PETROMAGNETIC STUDIES

The magnetic properties of two samples of the clay boundary layer are studied: from Gams-2A section (samples Nos.1–8 and 11) and the overlapping sandy-clayey deposits (samples 9, 12–16) (Fig. 1a) and from the Gams-2B section (samples 1–3 cover in more detail the bottom of the boundary layer, and sample 5 relates to its top (Fig. 1b)). For comparison the data on the magnetic properties of the boundary layer of the Gams-1B section are presented. The results of the sectional petromagnetic study are given in Tables 1 and 2. For comparison, the data on the magnetic properties of the boundary layer of Gams-1B section are presented.

The total concentration of magnetic minerals is expressed in the values M_s and M_{rs} (they behave concordantly (Figs. 3a and 3b)): in the Gams-2A section from below up to a level of 10 mm of the boundary layer the content of magnetic minerals rapidly increases and above it sufficiently smoothly drops. The lowest values of H_{cr}, M_{rs}/M_s, and H_{cr}/H_c (Fig. 3c, Tabl. 1) relate to the very bottom of the boundary layer. Above, H_{cr} smoothly increases within the limits of the boundary layer approximately from 20 to 100 mT.

The enumerated characteristics in the boundary layer of the Gams-1B section behave similarly (Fig. 3). Whereas in the Gams-2B section, which is located adjacent to the Gams-2A section, the bottom part of the section is apparently absent: the low values of M_{rs}, M_s,

Table 1. Magnetic properties of the samples of boundary layer and superincumbent deposits of the Gams sections

No.	mm	M_s	M_p	M_{rs}	M_{rs}/M_s	H_{cr}	H_c	H_{cr}/H_c
Gams-2A								
16	57	3.02	49.3	0.66	0.219	129.6	24.04	5.39
15	52	3.43	49	0.778	0.227	130.6	23	5.68
14	47	3.23	55.1	0.712	0.221	141.4	25	5.66
13	43	2.03	50.6	0.703	0.347	138.6	25.78	5.38
12	37	2.74	50.6	0.638	0.233	135.6	25.86	5.24
9	40	1.93	45.2	0.729	0.378	147.5	31.19	4.73
11	26	1.48	55.4	0.548	0.371	99.4	15.24	6.52
8	16	3.28	65.3	0.696	0.212	86.5	12.28	7.04
7	13	3.4	65	0.75	0.221	78.8	11.56	6.82
6	10	4.2	67.4	0.749	0.178	62.8	10.3	6.1
5	8	3.59	61.5	0.583	0.163	48.8	8.92	5.47
3	7	3.92	54.7	0.437	0.111	19.5	4.8	4.06
2	4	2.35	43.9	0.29	0.123	20.3	5.03	4.04
1	1	2.2	33.1	0.222	0.1	17.6	4.76	3.7
Gams-2B								
5	35	6.53	34.9	0.9	0.138	92.7	18.7	4.96
3	13	4.37	49.2	0.81	0.185	80.5	17.4	4.63
2	7	5.73	48.9	0.87	0.152	85.4	15.7	5.44
1	2	6.54	43.74	1.03	0.157	84.3	16.2	5.2
Gams-1B								
J_{top}	18	3.29	40	0.34	0.103	67.9	9.2	7.38
J_3	10	7.2	48.3	1.02	0.142	67.4	14.3	4.71
J_2	5	7.34	55.39	1.28	0.174	30.8	9.5	3.24
J_1	3	6.48	49	1.09	0.168	42	11.1	3.78
J_0	1	9.86	47.74	1	0.101	21.2	5.14	4.12

Note: No. is the sample number, mm is the distance from the bottom of the boundary layer in millimeters, M_{rs} is the specific remanent saturation magnetization, 10^{-3} A m^2/kg, M_s is the specific saturation magnetization, 10^{-3} A m^2/kg, M_p is the paramagnetic magnetization in the magnetic field of 500 mT at 20°C, 10^{-3} Am^2/kg, H_{cr} is the remanent coercive force in mT, H_c is the coercive force in mT.

H_{cr}, and their increase are absent (Fig. 3), i.e., the conditions of the accumulation of magnetic minerals were noticeably changed. The large ratios H_{cr}/H_c = 5–6 with the values M_{rs}/M_s = 0.22–0.38 (Table 1), are indicative of the considerable underestimation of H_c because of the presence of the large number of superparamagnetic particles [Pechersky et al., 2006].

The picture significantly changes on passing to the Danian sandy-clayey deposits of the Gams-2A section (samples 9, 12–16, Table 1). Here, the material in terms of its content, composition, and structural characteristics is very uniform, M_{rs} and M_s vary within fairly narrow limits (Table 1, samples 9, 12, 16, Figs. 3a and 3b), and the high coercivity (H_{cr} = 130–148 mT; M_{rs}/M_s = 0.22–0.23 (Table 1, Fig. 3b)) behaves stably approximately within the same interval, i.e., this is the size effect of fine high-coercivity magnetic grains, close to each other in their composition.

Differences in the coercivity of the rocks of the boundary layer and superincumbent sandy-clayey deposits of the Gams-2A and Gams-2B sections are clearly reflected in their coercive spectra. In Fig. 4a, the low maximum (region A) relates to the deposits of the boundary layer of the Gams-2A section. While passing to the Danian sandy-clayey deposits the high-coercivity maximum appears (region B). The Danian samples of

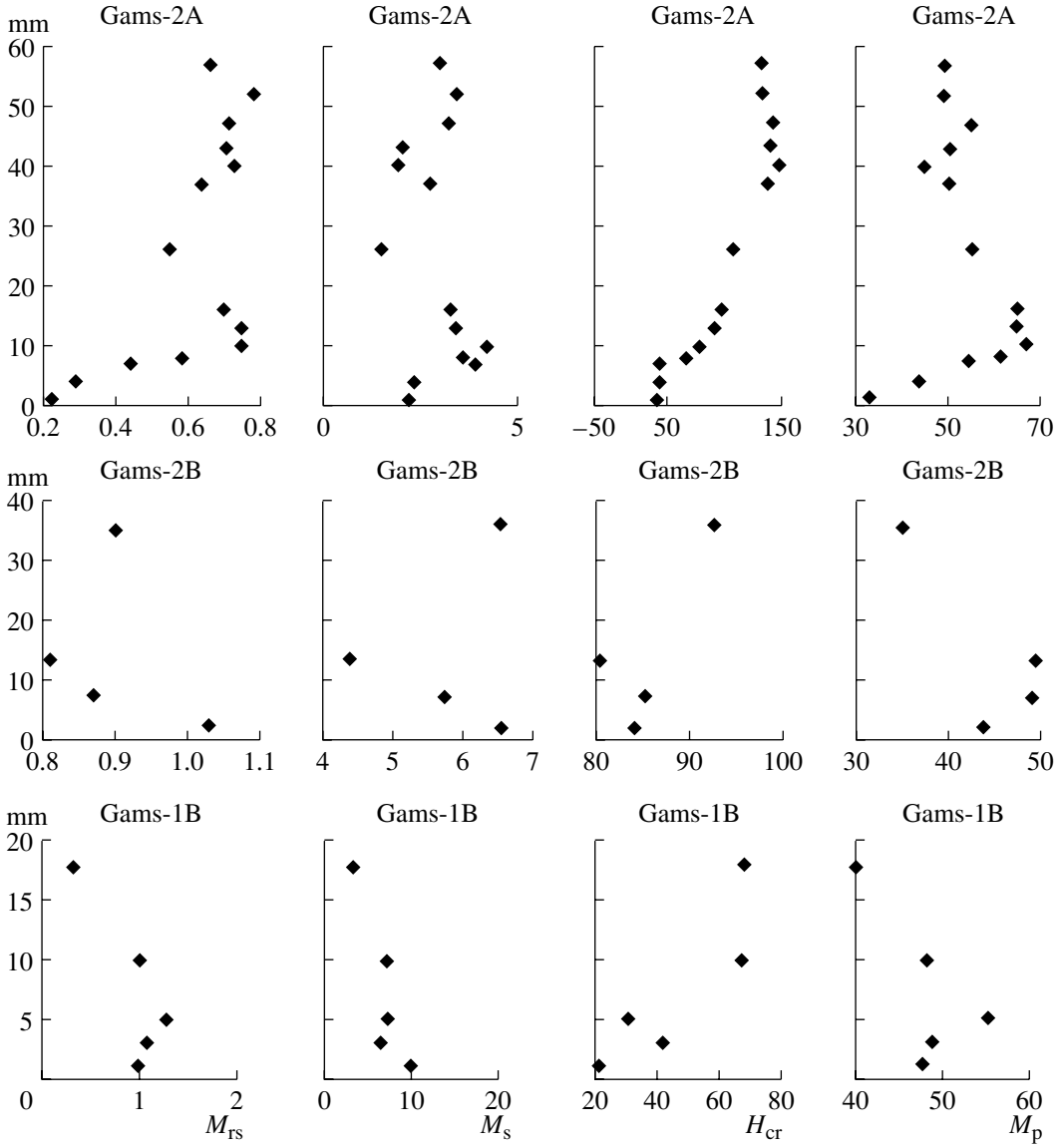

Fig. 3. Magnetic properties of the samples from the boundary layer and deposits overlapping it of the Gams-2A, Gams-2B, and Gams-1B.

the Gams-2A section have a common high-coercivity maximum (Fig. 4b). Such high coercivity is observed in the Danian sandy-clayey deposits of the Gams-1A section; however, its contribution to the coercive spectra of the boundary layer of the Gams-1A section noticeably falls (Fig. 4d) correspondingly, and the value H_{cr} falls from 90–120 to 50–60 mT [Pechersky et al., 2006].

The value of the paramagnetic magnetization M_p in the boundary layer of the Gams-2A section behaves very similarly to M_s and especially to M_{rs} (Fig. 3d), which is indicative of the joint accumulation of magnetic and paramagnetic minerals. The highest value of M_p falls on the same level of 10 mm (samples 6–8, Table 1), i.e., approximately there, where the maximum of the coercive spectra of the rocks of the boundary layer is located. The value of M_p is minimum at the very bottom of the Gams-2A section. Here, the lowest concentration of magnetic minerals is also observed both on M_{rs} and on M_s (Figs. 3a and 3b). Such a low drop in M_p in the Gams-1B and Gams-2B sections does not occur (Fig. 3d).

As can be seen from the data of thermomagnetic analysis (Table 2), the set of magnetic minerals of the Gams-2A and Gams-2B sections in composition and in content does not principally differ from the same in the boundary layer of the Gams-1 sections. The basic magnetic minerals, which are contained in the deposits of all three sections, are goethite, hemoilmenite, titanomagnetite, magnetite, and iron. The only exceptions are metallic nickel and its alloy with iron, discovered in the separate samples of the Gams-1 section. In turn, in the samples of the boundary layer of the Gams-1 section,

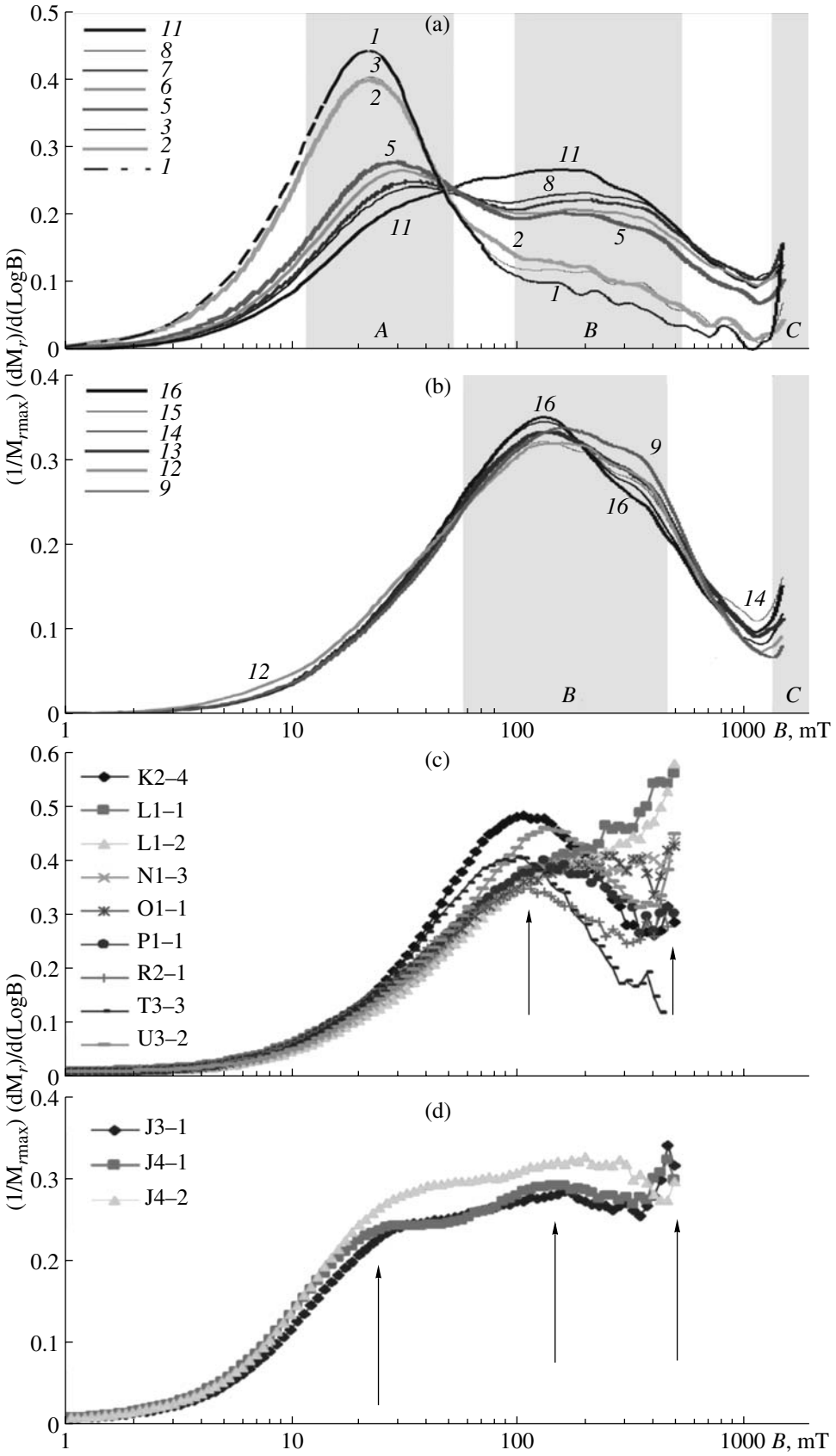

Fig. 4. Coercive spectra of the samples of (a), (b) the Gams-2A section and (c), (d) the Gams-1A section [Pechersky et al., 2006]; (a) and (c) the boundary layer; (b) and (d) the Danian deposits.

Table 2. Results of the thermomagnetic study of the samples from the boundary layer of the Gams sections

	First heating, T_c (fraction)							Secondary heating, T_c (fraction)							
Number	fsp (Ferrospinel)	Goethite	HI (Hemoilmenite)	Maghemite	MT (Magnetite)	M_{peak}	"Pyrite"	Hematite	Iron	fsp (Ferrospinel)	HI (Hemoilmenite)	TM (Titanomagnetite)	MT (Magnetite)	Hematite	M_t/M_0
Gams-2A															
1		130(15)	?	350	?	535(1.2)	595(400)	680(<5)	760(<5)		250	480?		675	1.47
2		130(14)		350	?	540(0.9)	590(240)	680(<5)	750(<5)		200	~500		675	1.06
3		140(16)	270?	~350	?	540(1.1)	590(260)	670(<5)			230	~490		670	1.08
5		130(13)	260?	330	?	540(0.85)	590(240)	670??		~150	?			670	1.46
6		130(13)	300	350	?	540(0.48)	540(0.48)	?		~150	250?	400		?	1.38
7		150(13)	250	320?	?	540(0.41)	590(120)	680(<5)			240?		570?	680	1.09
8		125(12)	250	300?	?	540(0.45)	590(150)	675(<5)		100	250		570?	675	1.09
9	130	130(4)	210	410	590(20)	0				130		530	575	675	0.99
11		120(11)	250	310	?	545(0.4)	590(130)	680??		150	250	510	580	680	1.14
12		140(6)	220?	300	590(10)	0		670??	760?		220	520?	570?	670	1.04
13		140(4)	230	300?	580(30)	0		660(<5)	770(<5)		180	520	570	670	0.93
14		140(5)	230	300?	580(30)	0		660(<5)	770(<5)		180	520	570	670	0.98
15		140(5)	230	300?	580(30)	0		660(<5)	770(<5)		180	520	570	670	0.95
16		120(4)	230?	390	585(30)	0		680??	760??		260	520	585	675	0.9
Gams-2B															
5		120(10)	230?	430	585(30)	0		680	0			510(< 5)	580	670	1.2
3		120(12)	270	330	?	545(0.4)	585(130)	670	0	100?		510(< 10)	580	670	1.13
2		120(10)	260	320	?	540(0.9)	590(260)	680(< 5)	0	100	250	510(25)	580(40)	680	1.6
1		130(8)	260	310	?	550(0.45)	590(140)	680?	750(<3)		220	520?	575	670	1.1
Gams-1B															
J_{top}		130(10)		350	0	0		660(20)*	740(10)			540(10)			0.88
J_3		130(12)	260	350	585(20)	?	?	0	0			510	580		1.08
J_2		130(10)	260	320	585(15)	0		0	750(<1)	H		410(20)	580		0.92
J_1		120(10)	250	380	580(20)	?	?	0	0	100?	270			660	0.98
J_0		130(10)		380	580(30)	0		680(< 3)	770(<1)?	160		460(25)	580		0.87

Note: No. is the sample number, T_c are the Curie temperatures, determined from the $M_i(T)$ curves of the first and second heating (in the case of maghemite this is the transition temperature in hematite), the fraction of magnetization, determined from the $M_i(T)$ curve as a result of extrapolation up to room temperature, is indicated within brackets in percents, fsp designates ferrospinel, HI designates hemoilmenite, MT designates magnetite, TM designates titanomagnetite, iron designates metallic iron, M_t / M_0 is the ratio of magnetization value, measured after the heating up to 800°C, to its initial value, M_{peak} is the temperature of the maximum on the $M_i(T)$ curve (the peak height relative to the initial M_i value is indicated in brackets), "Pyrite" is the Curie temperature of the newly formed magnetite (on "pyrite") during the laboratory heating of the sample (the magnetization value relative to the initial M_i value is presented in percentage in brackets), the results of extrapolation up to room temperature. The asterisk * designates FeNi-alloy.

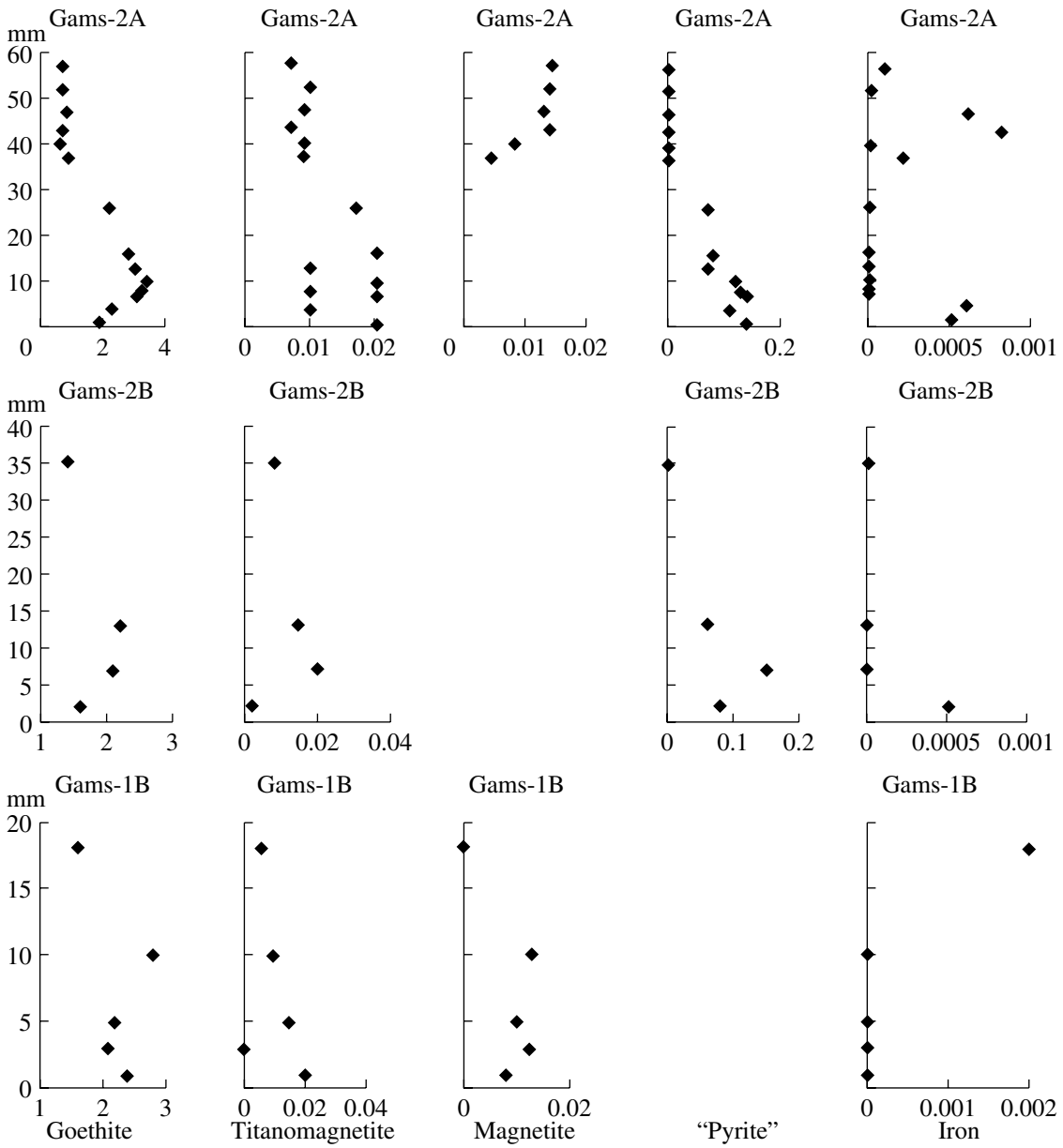

Fig. 5. Percentage composition of magnetic minerals in the Gams-2A, Gams-2B, and Gams-1B sections: goethite, titanomagnetite, magnetite, "pyrite" (the quantity of magnetite determined from "pyrite", formed in the process of laboratory heating of sample) and metallic iron.

Fe-sulfides of the pyrite type, which are present in noticeable quantities in the boundary layer of the Gams-2 sections, are not discovered.

The content of goethite (T_c ~ 100–180°C) in all sections (Fig. 5) practically repeats the behavior of paramagnetic magnetization: it smoothly increases from below reaching the maximum at a level of 10 mm, as well as M_p (Fig. 3d), and it smoothly falls in the upper part of the layer; passing to the Danian deposits it sharply falls up to 0.6–0.8% both in the Gams-1 section [Pechersky et al., 2006] and in the Gams-2 section (Fig. 5). Judging by the high coercivity, crystalline goethite predominates in the Danian deposits, and in the boundary clay a certain fraction of ochreous-earthy low-coercive goethite is possible, which is more noticeable in the Gams-2A section and which is almost absent in the Gams-2B section. Everywhere hemoilmenite (T_c = 200–300°C) and titanomagnetite (T_c = 400–530°C) are observed (Table 2). The titanomagnetite content is higher in the boundary layer in comparison with the Danian deposits and its distribution along the section is nonuniform (Fig. 5). Magnetite (T_c = 570–590°C) is not discovered in the boundary layer of the Gams-2B section because of the new growth of magnetite on the laboratory heat-

ing (see below). Metallic iron (T_c = 750–770°C) in the boundary layer of the Gams-2A, 2B, and 1B sections is not discovered except the very bottom itself, whereas in the layer of the Gams-1B section iron is discovered only in its upper part (Table 2, Fig. 5).

In the boundary layer of the Gams-2A and Gams-2B sections, as well as in the Gams-1A and Gams-1B sections, "ferrospinel" (T_c = 100–150°C) is encountered in separate samples (Table 2).

The boundary layer of the Gams-2A and Gams-2B sections sharply differs in terms of the thermomagnetic characteristics from the Gams-1 section. In the Gams-1 section the curves of $M_i(T)$ of the boundary layer and the superincumbent Danian deposits practically repeat each other. However, in the boundary layer of the Gams-2A and Gams-2B sections, a peak at 540 ± 5°C appears on the curve of $M_i(T)$. The height of this peak is the maximum at the bottom of the boundary layer of the Gams-2A section, is slightly higher in the boundary layer of the Gams-2B section, and regularly falls with the approach of the Danian deposits and is almost absent in the Danian deposits (Table 2, Fig. 6). After the peak the decrease of the curve of $M_i(T)$ is completed at the Curie point (590–595°C), i.e., in the course of laboratory heating oxidized magnetite is formed (Fig. 6). With further heating of the sample up to 800°C, the magnetite is oxidized to hematite, which is evident on the curve of $M_i(T)$s. As a result, an appreciable part of the newly formed magnetite is destroyed and it hardly remains on the curve of $M_i(T)$ of reheating. The peak becomes appreciably obscure within the temperature range 500–600°C. Thereby, on the curves of $M_i(T)$ of the first heating of the rocks of the Gams-2A and Gams-2B sections natural magnetite and titanomagnetite are not observed, being frequently encountered in the samples of the Gams-1 section outside of the boundary layer [Pechersky et al., 2006] and within its limits, whose content widely varies from the absence to 0.01–0.02%. Judging by the curves of $M_i(T)$ of the second heating, titanomagnetite in the Gams-2 section, as well as in the Gams-1 section, is observed almost throughout the entire boundary layer (Fig. 5, Table 2). Magnetite is confidently identified only in the Danian deposits of the Gams-2A section, where it is not "screened" by the newly formed magnetite in the process of laboratory heating (Fig. 5). Due to the latter, northing can be said about the presence of the natural magnetite in the boundary layer of the Gams-2B section. Indirectly, the clear inverse correlation of H_{cr} with the peak height on the curve of $M_i(T)$ (Fig. 7) indicates its presence in the Gams-2A section. Judging by the noticeable predominance of the low-coercive material (the coercive spectra and H_{cr}), the quantity of magnetite in the boundary layer of the Gams-2A section is substantially higher than in the superincumbent Danian deposits.

It would be logical to relate the appearance of magnetite in the course of laboratory heating with the presence in the the samples of the boundary layer, especially in its bottoms, of iron sulfides, such as pyrite and arsenopyrite, observed in this layer according to mineralogical observations (the data of A.F. Grachev). Magnetite usually appears on heating such minerals to higher than 500°C and is considered as the diagnostic criterion of pyrite and arsenopyrite [Novakova and Gendler, 1995]. Accordingly, one can easily assume that a certain quantity of magnetite of the order of 0.05% on Fe-sulfides was present before the laboratory heating of the samples of the Gams-2A section. The relatively high coercivity of the samples of the Gams-2B section (H_{cr} = 80–93 mT) is indicative of the low magnetite content in them before heating, whereas the peak on $M_i(T)$ implies the presence of Fe-sulfides of the pyrite type in the Gams-2B section also. The quantity of the newly formed magnetite, obviously, reflects the quantity of Fe-sulfides ("pyrite"). If we extrapolate by parabola the decay curve of $M_i(T)$ higher than 500°C up to room temperature, then from this value it is possible to determine the quantity of the newly formed magnetite on "pyrite". If we assume that all "pyrite" was oxidized to magnetite, then from the magnetization value of the newly formed magnetite, we can determine the content of the initial "pyrite", or more precisely, it will be the lower limit of the possible "pyrite" content in the sample. Such estimates are presented in Fig. 5. Obviously, the grains of "pyrite" are very small, judging by the fact that they were so easily oxidized to magnetite and, then, the newly formed magnetite could be oxidized to hematite even during the first heating up to 800°C.

Metallic iron with a low concentration (less than 0.001%) is present in the Danian deposits of the Gams-2A section and is scarcely encountered in the boundary clay both in the Gams-1 and Gams-2 sections (Figs. 5 and 8). It is important to emphasize: in the boundary layer near the Cretaceous/Tertiary boundary, metallic iron is scarcely encountered, but it, most likely, has a meteoritic origin. This means that precisely at this time impact events are improbable.

Now, we shall consider the relationship of the $M_p$value and concentrations of magnetic minerals in the boundary layer. As is known, the concentration distribution of minerals, elements and so on is governed by the log-normal law. Therefore, it is more suitable and more visible to consider the comparison of such factors on a logarithmic scale (Fig. 8). Both in all the sediments studied (Fig. 2) and in the boundary clay a clear direct correlation between the M_p value and the goethite content is observed (Fig. 8). At the same time the contents of magnetite, titanomagnetite, and metallic iron do not correlate at all with the content of the iron hydroxides (Fig. 8). This counts in favor of the independent accumulation conditions of the minerals enumerated and, obviously, of their different sources.

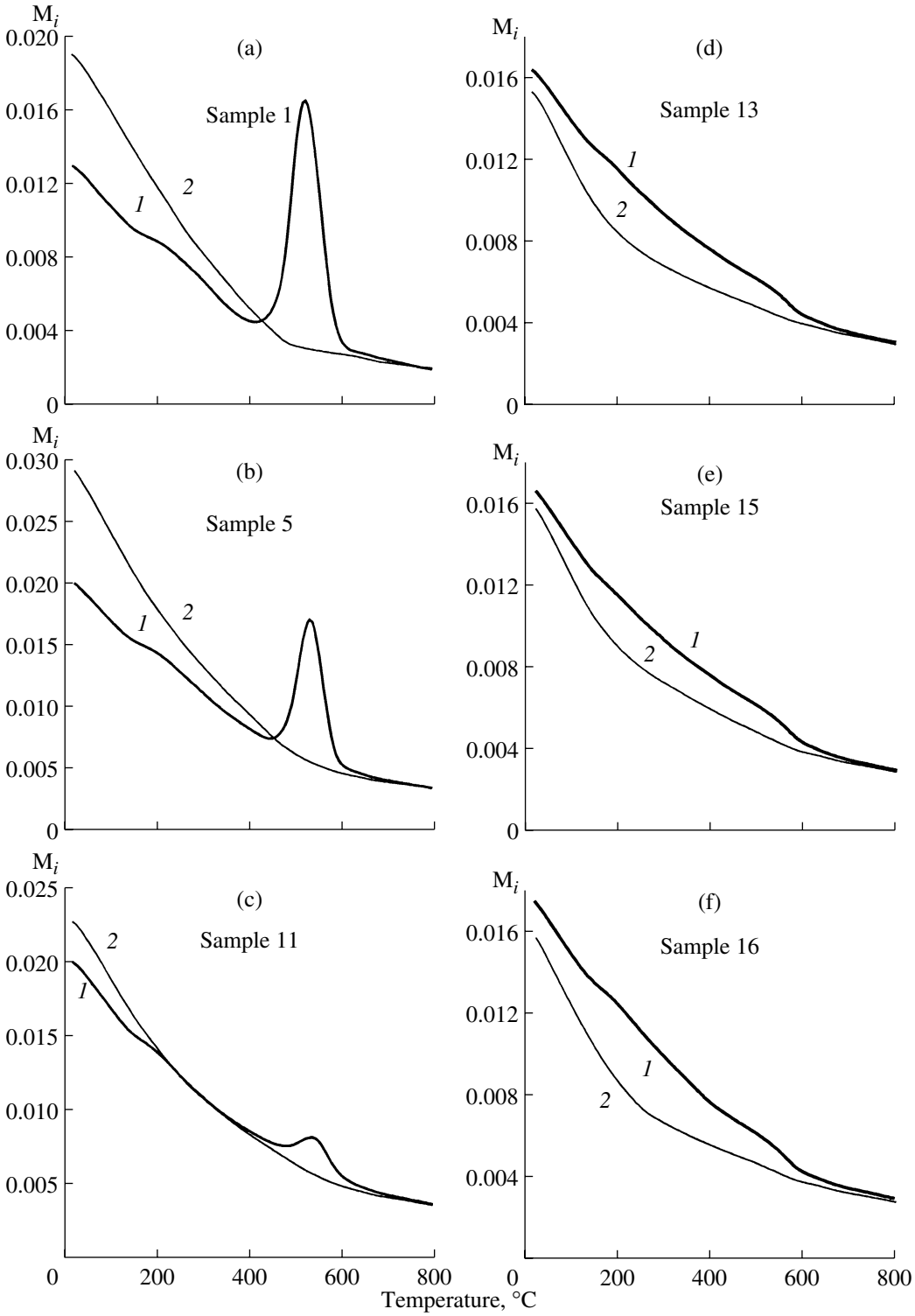

Fig. 6. Examples of M_i(curves of the samples from (a), (b), (c) the boundary clay and (d), (e), (f) the Danian deposits of the Gams-2A section).

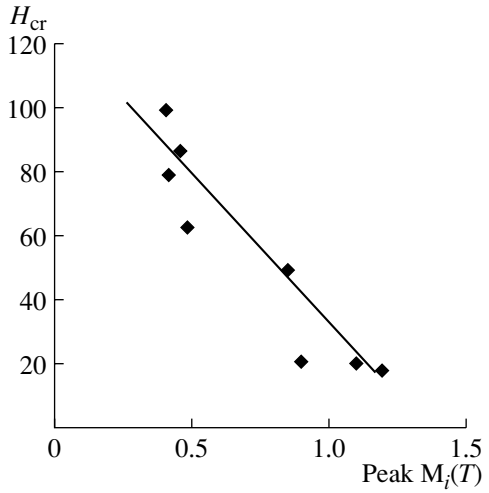

Fig. 7. Correlation of the relative peak height on the $M_i(T)$ curve and H_{cr}, the Gams-2A section.

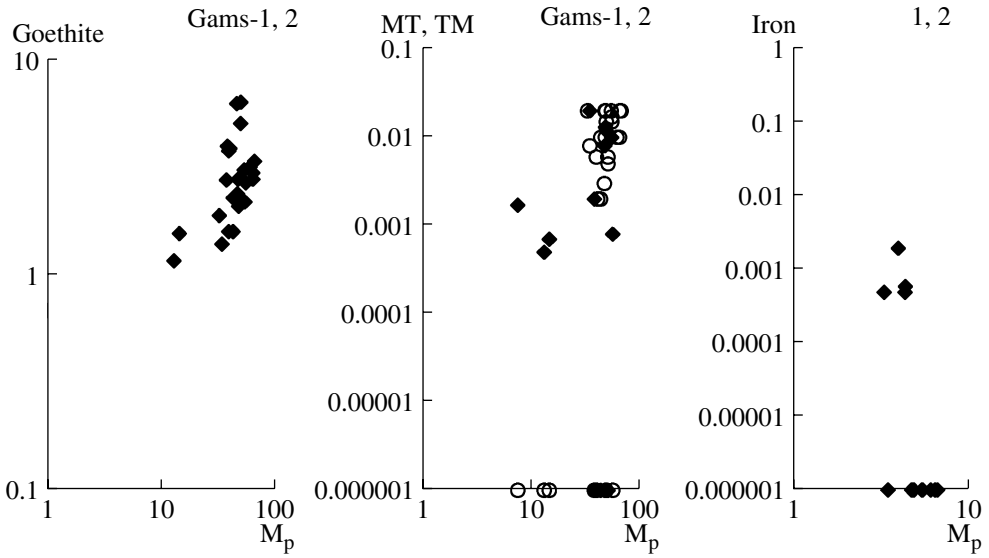

Fig. 8. Correlation between the paramagnetic magnetization and the percentage composition in the boundary layer (the Gams-1 and Gams-2 sections) of goethite, magnetite, titanomagnetite (open circles), and metallic iron.

CONCLUSIONS

The analysis of petromagnetic data on the boundary layer of the Gams-1 and Gams-2 sections makes it possible to make the following conclusions.

(a) The composition of basic magnetic minerals in the boundary layer of the Gams-1A and the Gams-1B, as well as the Gams-2A and the Gams-2B sections is similar: these are hydroxides of iron, hemoilmenite, titanomagnetite, magnetite, hematite, and metallic iron.

(b) The difference consists in the presence in the boundary layer of the Gams-1 section of metallic nickel and its alloy with iron and in the absence of iron sulfides in it, whereas in the Gams-2 section nickel is not identified, instead, Fe-sulfides of the pyrite type are present. This implies the locality of the distribution of the minerals mentioned above.

(c) The content of Fe-sulfides of the pyrite type, determined from the peak value on the thermomagnetic curves inside the boundary layer in the two Gams-2A and Gams-2B sections, is maximal at the bottom of the boundary layer and is regularly reduced upwards. In the Danian deposits above the boundary layer Fe-sulfides are absent. The clear inverse correlation of the remanent coercive force, which characterizes the state of the magnetic grains in the samples before their laboratory heating, and a sharp increase in the magnetization during the laboratory heating of the samples from the boundary layer of the Gams-2A and Gams-2B sections

imply that the low-coercive material, determined from both the H_{cr} value and the coercive spectrum, is magnetite, which is closely related to Fe-sulfides. By analogy, it is possible to assume that the low-coercive material in the lower part of the boundary layer of the Gams-1B section is also magnetite. Earlier we related it to the presence of nickel.

(d) At the bottom of the boundary layer of the Gams-1A section noticeable enrichment by titanomagnetite and ilmenite is observed, with the compositions, characteristic for basalts. Above the boundary layer, their content sharply falls up to a certain background level. In the Gams-1B and 2A sections this enrichment of the bottoms of the boundary layer by titanomagnetite is not recorded. Here, in the entire layer the content of titanomagnetite varies within narrow limits (0.01–0.02%). Hence, it is possible to conclude that the precipitation of titanomagnetite particles, related to the volcanic eruption, occurs very unevenly.

(e) Only the concentration of iron hydroxides behaves monotonously in the Gams-2A, 2B, and 1B sections: being the lowest in the very bottom of the boundary layer, it stably grows to a maximum at a level of ~10 mm and then it smoothly decays. Consequently, near the Cretaceous/Tertiary boundary, a pronounced accumulation of iron hydroxides occurs and, as shown by the data on a series of sections [Pechersky, 2007], this is probably a global effect. It is irrelevant to the local physicogeographical characteristics of the accumulation of terrigenous material in sediments. Apparently, the accumulation of the main body of iron hydroxides in the boundary layer and in the remaining deposits have a different nature. Thus, between the total effect of accumulation of magnetic minerals ($M_s$and M_{rs}) and of paramagnetic minerals (M_p) in sediments the correlation is absent, reflecting the different nature of their accumulation (mainly terrigenous), whereas in the boundary layer of this correlation is clearly visible, which is possible to explain by the common or close nature of the accumulation of both magnetic and paramagnetic minerals in the boundary clay, and ferromagnetic and paramagnetic iron hydroxides, the main contributors in M_s, M_{rs}, and M_p, respectively. We relate this to the predominantly hydrothermal nature of iron hydroxides in the boundary layer, resembling somewhat the metal-bearing sediment type [Gurvich, 1998]. The accumulation of iron hydroxides is extended in time, reaching a maximum in the lower third of the boundary layer, and is sharply reduced upon passing into the overlying and underlying Danian and Maastrichtian deposits. At the same time, the absence of the correlation of the contents of magnetic minerals, such as magnetite, titanomagnetite and metallic iron, with the content of iron hydroxides indicates the different sources of their accumulation in the layer of boundary clay.

Thus, only the enrichment by iron hydroxides, apparently, of the common origin, can be considered as a global, natural phenomenon, related to the Cretaceous/Tertiary boundary and irrelevant to the impact events.

(f) In connection with the problem of the nature of the boundary layer near the Cretaceous/Tertiary boundary, it is important to emphasize that the criterion of impact events such as the particles of metallic iron, according to all indications of meteoritic origin, are almost absent in the boundary layer. They are identified in the upper part of the boundary layer of the Gams-1B and 2A sections and at the bottom of the boundary layer of the Gams section, i.e., at completely different time levels.

The jump in the accumulation of titanomagnetite at the bottom of the boundary layer of the Gams-2A and the Gams-2B sections is irrelevant to the impact events, whose attributes (the appearance of metallic nickel and alloy with iron and the anomaly of the iridium content) fall to the tops of the boundary layer, but the increased content of iron hydroxides is "stretched" over the entire boundary layer. Fe-sulfides appear at the bottoms of the layer of the boundary clay, and their quantity gradually decreases towards the top of the layer, which also cannot be related to the impact event. What is more, a sharp increase in the content of iron hydroxides is observed in all known sections, whereas metallic nickel is identified only in the Gams-1 section. Consequently, the Cretaceous/Tertiary boundary is not characterized by the direct attributes of an impact event.

REFERENCES

1. Sh. Adamia, N. Salukadze, M. Nazarov, G. Gongadze, O. Gavtadze, E. Kilasonia, and A. Asanidze, "Geological Events at the Cretaceous-Paleogen Boundary in Georgia (Caucasus)," Geologica Carpatica **23** (3), 35–43 (1993).
2. B. V. Burov, D. K. Nurgaliev, and P. G. Yasonov, *Paleomagnetic Analysis* (Izd. KGU, Kazan, 1986), pp. 1–167 [in Russian].
3. A. F. Grachev, O. A. Korchagin, H. A. Kollmann, D. M. Pechersky, and V. A. Tselmovich, "A New Look at the Nature of the Transitional Layer at the K/T Boundary near Gams, Eastern Alps, Austria, and the Problem of the Mass Extinction of the Biota," Russ. J. Earth Sci. **7** (ES6001. doi:10.2205/2005ES000189) (2005).
4. E. G. Gurvich, *Metalliferous Sediments of the World Ocean* (Nauchnyi mir, Moscow 1998), pp. 1–337 [in Russian].
5. R. Lahodynsky, "Lithostratigraphy and Sedimentology across the Cretaceous/Tertiary Boundary in the Flyschgosau (Eastern Alps, Austria)," Riv. Espanola de Paleontologia, No. Extraordinario, 73–82 (1988).
6. E. A. Molostovsky, V. A. Fomin, and D. M. Pechersky, "Sedimentogenesis in Maastrichtian-Danian Basins of the Russian Plate and Adjacent Areas in the Context of Plume Geodynamics," Russ. J. Earth Sci. **8** ES6001. doi:10.2205/2006ES000206 (2006).
7. A. A. Novakova and T. S. Gendler, "Metastable Structural-Magnetic Transformations in Sulfides in Course of

Oxidation," J. of Radioanalyt. and Nuclear Chem. **190** (2), 363–368 (1995).

8. D. M. Pechersky, "Enrichment of Sediments in Iron Hydroxides at the Mesozoic-Cenozoic Boundary: A Synthesis of Petromagnetic Data," Fiz. Zemli, No. 3, 65–72 (2008) [Izvestiya, Phys. Solid Earth **44**, 232–238 (2008)].
9. D. M. Pechersky and A. V. Garbuzenko, "The Mesozoic-Cenozoic Boundary: Paleomagnetic Characteristic," Russian J. Earth Sci. **7** (2), (2005).
10. D. M. Pechersky, A. F. Grachev, D. C. Nourgaliev, V. A. Tselmovich, and Z. V. Sharonova, "Magnetolithologic and Magnetomineralogical Characteristics of Deposits at the Mesozoic/Cenozoic Boundary: Gams Section (Austria)," Russ. J. Earth Sci. **8** (3), ES3001. doi: 10.2205/2006ES000204 (2006).
11. D. M. Pechersky, D. C. Nourgaliev, Z. V. Sharonova, "Magnetolithologic and Magnetomineralogical Characteristics of Deposits at the Mesozoic/Cenozoic Boundary: Koshak Section (Mangyshlak)," Russ. J. Earth Sci., No. 11, 99–112 (2006).
12. L. E. Sholpo, *Application of Rock Magnetism for Solution of Geological Problems* (Leningrad, Nedra, 1977), pp. 1–182 [in Russian].
13. S. V. Vonsovskii, *Magnetism* (Nauka, Moscow, 1971), pp. 1–1032 [in Russian].
14. P. G. Yasonov, D. C. Nourgaliev, B. V. Bourov, F. Heller, "A Modernized Coercivity Spectrometer," Geologica Carpathica. **49** (3), 224–226 (1998).